Revista Tecnológica - Universidade Estadual de Maringá - ISSN 1517-8048
DOI: 10.4025/revtecnol.v29i2.52653

CALCULATION OF STRESS CONCENTRATION FACTORS OF PLATES UNDER TENSION VIA COMPUTER PROGRAM DEVELOPED

CÁLCULO DE FATORES DE CONCENTRAÇÃO DE TENSÃO DE CHAPAS SOB TRAÇÃO POR MEIO DE PROGRAMA DE COMPUTADOR DESENVOLVIDO

Raphael Basílio Pires Nonato[1]

Abstract: Stress concentration factors (SCFs) for some set of fixed geometrical and loading cases can be obtained experimentally, analytically, and computationally. To accomplish this, tables and charts that relate a geometrical ratio and a specific type of loading with their correspondent SCF are available. Although these resources are accessible for the most common cases, their reading and interpretation processes often imply parallax error. To overcome this difficulty, the interpolated equations may be applied. However, the application of the adequate equation in a non-structured manner can be time consuming within a whole design process. Thus, the study of two geometrical cases of plates under tension in elastic range enabled the comparison of SCFs obtained from three sources: (a) chart reading; (b) approximate proven equations; and (c) specific computer program developed by the author in Microsoft Visual Basic 6.0®. The relative error between the SCFsextracted from the software and those from the charts presentedvalues up to 1.786% and 2.588% for the first and second cases, respectively. Additionally, a total agreement up to the third decimal placewas reached between interpolated equations used in the developed software and equations presented by some authors, which validates the software in the applied domain.
Keywords: Stress concentration factor. Software. Tension. Plate.

Resumo:*Fatores de concentração de tensão (FsCT) podem ser obtidos experimental, analítica e computacionalmente para alguns conjuntos de casos fixos de geometria e carregamento. Com vistas a obter estes fatores, tabelas e gráficos que relacionam uma razão geométrica e um tipo de carregamento específico com seu FCT correspondente estão disponíveis. Apesar de estes recursos estarem disponíveis para os casos mais comuns, o processo de leitura e interpretação destas fontes frequentemente implicam em erros de paralaxe. De modo a transpassar esta dificuldade, as equações aproximadas ou interpoladas podem ser aplicadas. Contudo, a aplicação da equação adequada de um modo não estruturado pode consumir tempo além do previsto no processo de projeto como um todo. Deste modo, o estudo de dois casos geométricos de chapas sob tração na região elástica permitiu a comparação de FsCT obtidos de três maneiras: (a) leitura de gráfico; (b) equações provadas aproximadas; (c) programa de computador específico desenvolvido pelo autor no Microsoft Visual Basic 6.0®. O erro relativo entre os FsCT extraídos do programa e aqueles dos gráficos apresentou valores até 1.786% e 2.588% para o primeiro e segundo casos, respectivamente. Adicionalmente, total concordância até a terceira casa decimal foi conseguida entre as equações de interpolação usadas no programa e as apresentadas por alguns autores, o que valida o programa no domínio aplicado.*
Palavras-chaves:*Fator de concentração de tensão. Programa de computador. Tração. Chapa.*

[1]*CEFET-RJ- Centro Federal de Educação Tecnológica Celso Suckow da Fonseca, email: raphaelbasilio@gmail.com*

Revista Tecnológica - Universidade Estadual de Maringá - ISSN 1517-8048
DOI: 10.4025/revtecnol.v29i2.52653

1 Introduction

Stress concentration factors (SCFs) are part of analysis scope of common engineering parts. Since SCFs are mainly due to load application and/or sudden change in geometric form of machine elements (particularly called Form Stress Concentration Factors, FSCFs), practically, these factors are frequently being evaluated to obtain the maximum actuating stress on each analyzed region(Pilkey et al., 2020).

For some set of fixed geometrical and loading conditions, the FSCFs can be obtained experimentally (e.g., photoelasticity or strain gages), analytically (e.g., elasticity theory), or computationally (e.g., Finite Element Method, FEM). From specific tables and charts built experimentally or from their related mathematical expressions (interpolated equations), the correspondent FSCFs are often extracted (Muminovic et al., 2014).

Commercial packages (e.g., Ansys®, Nastran®, Abaqus®, Lisa®, etc.) grounded on some of the existing numerical methods are already available for this type of calculation. However, in most of the cases, the access to this type of software implies investment in expensive licenses, which is not feasible for small private companies, universities, and some institutions, for example.

In the case of extracting the factors from the referred charts as a simple process of manual data reading, it is known that one of the common problems faced is the parallax error. The reading process of the pertinent values rarely incurs in an undoubted value referred to the accuracy needed. This process brings a relative imprecision because of its manual (visual) manner of determination.

On the other hand, even when the case allows the obtainment of the stress concentration factor via an approximate numericalmethod, which is the case of some expensive softwares already mentioned, an unorganized process can produce execution errors besides being time consuming in the sense of non-organized method of accomplishment.

The more general problem of finding an alternative to the imprecision of reading experimental charts and to the referred expensive specific softwares has led some researchers to dedicate themselves to find the corresponding solutions in terms of contributions of developed computer programs to solve for the FSCFs (Jr.;Shahhosseini, 2002;Muminovic et al., 2014; Kmecz, 1972; Kannan, 2018); and computer programs simply used to compare the calculated factors with those obtained by other manners (Muminovic et al., 2015; Gunwant et al., 2016; Santos et al., 2016; Bidhar et al., 2015;Ozkan; Toktas, 2016; Pathak et al., 2018).

In Jr.;Shahhosseini(2002), the authors developed a Windows-based computer program for the calculation of FSCFs for a wide variety of geometry and load cases. The software created inside Microsoft Visual Basic 6.0 allows the user to choose between two measurement systems: *SystèmeInternationale* (SI) and United States Customary System (USCS). Besides calculating the FSCFs, stresses are also obtained with the possibility of saving critical point configuration and latter recalling it.

Muminovic et al. (2014) developed a Windows-based software to which another results from other computer programs are compared. In addition to the created software, the authors performed an analysis based on the literature using modules inside Microsoft Excel. An interpolation technique provided approximate equations to the calculation of FSCFs. Microsoft Visual Basic was emulated within Microsoft Visual Studio to output FSCFs, nominal, and maximum stresses.

Kmecz (1972) created a computer program to obtain stresses (by means of the FSCFs) and deformations within axisymmetric structures of arbitrary shape. Temperature changes, gravity forces, and concentrated loads are input data to calculate the effects of stress or

Revista Tecnológica - Universidade Estadual de Maringá - ISSN 1517-8048
DOI: 10.4025/revtecnol.v29i2.52653

displacement boundary conditions. In addition, a successive approximation technique included non-linear material properties.

Kannan (2018) showed the calculation of FSCFs for axial, in-plane, and out-of-plane in the fatigue life of tubular joints. Computer program results were compared with the corresponding analytical.

Muminovic et al. (2015) calculated the FSCFs inside a commercial package of FEM and compared to the results collected from the software already mentioned here, developed by Muminovic et al. (2014). Thus, the created program could be investigated in what concerns to its accuracy.

The works of Gunwant et al. (2016) and Santos et al. (2016) have both determined the FSCFs by applying the FEM. The first studied flat plates with eccentric circular and elliptic holes under tension. In addition, they have analyzed the stress distributions around double semicircular notches. The second work focused on flat plates with combined discontinuities, comparing values obtained via equations with those from the FEM in order to validate the use of the FEM commercial package.

An empirical mathematical expression for the FSCF was obtained in (Bidhar et al., 2015) for an unequal-sized cavity pair in an arbitrary orientation. Finite Element Analyses (FEAs) were performed to verify the behavior of FSCFs for different orientations, sizes, and separation of cavities. The empirical formula is proposed to be applied as a guideline for selecting a casting method for car engine blocks in what refers to fatigue crack initiation.

Ozkan and Toktas (2016) and Pathak et al. (2018) both determine the FSCF using different methods to compare the results obtained from different manners. The former referred work compares the empirical FSCF with those obtained by analytical, regression analysis, FEA, and artificial neural network. The latter work established FSCFs of a round bar with "u"-groove via: (a) FEM; (b) chart experimentally obtained (extracted from a book); and (c) experiment (using the universal testing machine), and compared the results.

From the books cited (Young;Budynas, 2002; Budynas-Nisbett, 2008; and Pilkey et al., 2020), charts relating the FSCF with its pertinent geometrical factor were consulted for the cases calculated on the software presented in this paper. For several situations, there are also the mathematical expressions (commonly interpolated) originated from the experiments performed to construct these charts.

Therefore, in this paper, a Windows-based software is proposed in place of the well-known tables, charts, and expensive commercial packages in the context of FSCFs calculation of plates under tension. The referred software provides two sets of geometrical and tensile loading situations (cases). Complementarily, the program calculates the nominal and the maximum stresses for both cases. An approximate equation was obtained via interpolation (by Lagrange's method) of the discrete points of the charts for each geometric type of discontinuity and the results for the FSCFs provided by the software were validated through the comparison with the approximate proven equations developed by two authors (Howland (1930) for the first case and Ling (1968) for the second case). This comparison showed a good accuracy in the range within the valid domain of equation. Additionally, a comparison through the relative error between the results obtained by the software and those read from charts presented discrepancy.

2 Stress Concentration and Software Solutions

This section shows the contextualization related to the stress concentration phenomenon and its formulation, emphasizing the difference between the two basic types of FSCFs. The strategy of interpolation to create an approximate equation to model the FSCF as

Revista Tecnológica - Universidade Estadual de Maringá - ISSN 1517-8048
DOI: 10.4025/revtecnol.v29i2.52653

a function of the pertinent geometric factor is presented and two cases of plates under tension are studied.

2.1 Stress Analysis

The failure of an engineering part is commonly started at its weakest points, where either a damage (e.g., a micro crack) is caused by the impurity of the crystalline material or the magnitude of actuating stress is larger than the corresponding strength. In the process of development of basic elastic stress formulation (only elastic range is considered in this work), no stress concentration is then assumed. This is referred to the calculation of the actuating stresses on a prismatic bar which cross-section is far enough from the point or region of load application (Saint-Venant's principle assumption). Under this scenario, the stress concentration phenomenon due to loading application is simply neglected. This is mainly due to the analysis objective, which is particularly to find the nominal stress(Pilkey et al., 2020).

However, in engineering design, geometric discontinuities frequently exist in almost every component due to its functionality within the context of the corresponding assembly. Grooves, holes, keyways, shoulders, threads, cracks, etc. are a few examples of discontinuities, which address the concept of stress concentration phenomenon, quantified by the so-called stress concentration factor (Young;Budynas, 2002).

Related to the accuracy of stress calculation, analytical solutions for this type of problem are based on the formulations of the theory of elasticity, which include assumptions such as the homogeneity of the material, isotropy, and defect-free. In a more reliable analysis, an approach considering a more realistic material model could be adopted (Budynas-Nisbett, 2008).

2.2 Stress Concentration Factors

The mentioned discontinuities change stress distribution as the stress "flow" from a region with constant geometric characteristics through a discontinuity. Thus, when the comparison between stress and strength is made, it is imperative to evaluate how a geometric discontinuity increases the stress at this region by the stress concentration phenomenon. Therefore, stress concentration in elastic range means the localized stress higher than the nominal stress, which occurs due to a geometric discontinuity. To quantify how larger is the peak of stress related to its nominal, the stress concentration factor (SCF) quantity is introduced, which is expressed by K_t (theoretical) in Equation 1 (Young;Budynas, 2002),

$$K_t = \frac{\sigma_{max}}{\sigma_{nom}}, \tag{1}$$

where σ_{max} represents the maximum actuating normal stress in the part and σ_{nom} is the nominal or mean actuating normal stress. The same concept could be applied to define the SCF for shear stress, but stresses of this nature are not the focus of this paper. Also, the SCF treated here is not due to the application of a loading system, but referred to geometric discontinuities, thus receiving the nomenclature of form stress concentration factor (FSCF).The geometric discontinuity addresses that the nominal stress can be determined in the following two manners:

(a) if the gross cross-sectional area A_g (cross-section far enough from any discontinuities) is considered, then the nominal stress in Equation 2 holds:

Revista Tecnológica - Universidade Estadual de Maringá - ISSN 1517-8048
DOI: 10.4025/revtecnol.v29i2.52653

$$\sigma_{nomg} = \frac{P}{A_g}\ ; \tag{2}$$

(b) if the net cross-sectional area A_n (cross-section at the discontinuity studied) is now used, Equation 3 applies:

$$\sigma_{nomn} = \frac{P}{A_n}, \tag{3}$$

where P is the magnitude of the tensile loading system, σ_{nomg} is the gross nominal stress applied to the solid being analyzed, and σ_{nomn} is the net nominal stress. Therefore, the corresponding FSCFs, one considering the gross cross-section, and the other calculated assuming the net cross-section are, respectively, given by Equations 4 and 5:

$$K_{tg} = \frac{\sigma_{max}}{\sigma_{nomg}}\ ; \tag{4}$$

$$K_{tn} = \frac{\sigma_{max}}{\sigma_{nomn}}. \tag{5}$$

In this paper, FSCFs are given by the concept of Equation 5, i.e. K_{tn} (see Equation 6). Therefore, Equation 7 gives the maximum stress. They are presented by:

$$FSCF = K_{tn}\ ; \tag{6}$$

$$\sigma_{max} = K_{tn}\sigma_{nomn}\ . \tag{7}$$

To overcome the difficulty of interpretation in the reading process of an experimental curve or the execution of the calculation in a non-organized manner, this paper implements an interpolation function via Lagrange's method applied in the software developed. In a general character, the interpolating polynomial $P(x)$ of degree *n-1* with *n* terms through the *n* points is defined by the Lagrange's classical formula (Equation 8):

$$\begin{aligned} P(x) = {} & \frac{(x-x_1)(x-x_2)\cdots(x-x_{n-1})}{(x_0-x_1)(x_0-x_2)(x_0-x_{n-1})}y_0 \\ & + \frac{(x-x_0)(x-x_2)\cdots(x-x_{n-1})}{(x_1-x_0)(x_1-x_2)(x_1-x_{n-1})}y_1 + \cdots \\ & + \frac{(x-x_0)(x-x_1)\cdots(x-x_{n-2})}{(x_{n-1}-x_0)(x_{n-1}-x_1)(x_{n-1}-x_{n-2})}y_{n-1}\ , \end{aligned} \tag{8}$$

where the n points are defined by $y_0 = f(x_0), y_1 = f(x_1), \cdots, y_{n-1} = f(x_{n-1})$.In this context, $y_0, y_1, \cdots, y_{n-1}$ are the FSCFs and *x* is the geometric factor.

When the interpolation uses the number of coefficients equal to the number of tabulated values, the interpolation function gives the tabulated values perfectly. Therefore, to obtain the matrix of the coefficients c_i of the interpolated equation, Equation 9 is run. Adjacent to this matrix, in the left side of equation, matrix of x_i is known as a Vandermonde matrix (geometric progression in each row and the right side of Equation 9 is represented by the matrix of y_i.

Revista Tecnológica - Universidade Estadual de Maringá - ISSN 1517-8048
DOI: 10.4025/revtecnol.v29i2.52653

$$\begin{bmatrix} x_0^0 & x_0^1 & x_0^2 & x & x_0^{n-1} \\ x_1^0 & x_1^1 & x_1^2 & x & x_1^{n-1} \\ \vdots & \vdots & \vdots & \ddots & \vdots \\ x_{n-1}^0 & x_{n-1}^1 & x_{n-1}^2 & x & x_{n-1}^{n-1} \end{bmatrix} \begin{bmatrix} c_0 \\ c_1 \\ \vdots \\ c_{n-1} \end{bmatrix} = \begin{bmatrix} y_0 \\ y_1 \\ \vdots \\ y_{n-1} \end{bmatrix}. \quad (9)$$

If the tabulated points are represented by $y_i \equiv y(x_i)$, where i is the i-th tabulated point, the interpolating polynomial can be written by Equation 10:

$$P(x) = f(x_0)L_0(x) + \cdots + f(x_{n-1})L_{n-1}(x) = \sum_{i=0}^{n-1} f(x_i)\, L_i(x)\,, \quad (10)$$

where the term $L_i(x)$ is given by Equation 11:

$$L_i(x) = \prod_{k=0,\ k\neq i}^{n-1} \frac{x - x_k}{x_i - x_k}. \quad (11)$$

Although there are more efficient methods, Equation 9 can also be solved by standard techniques for linear equations. A timely observation to make is about the Vandermonde matrix, which will determine if the system is solvable through the non-nullity of its determinant.

2.3Plate with Central Hole under Tension

An example of such a case of transition between a constant cross-section and a discontinuity is a plate (strip) with a central hole. When this part is under a homogeneous tensile loading system applied far enough from the discontinuity, the stress distribution is similar to the profile shown around each side of the hole in Figure 1.

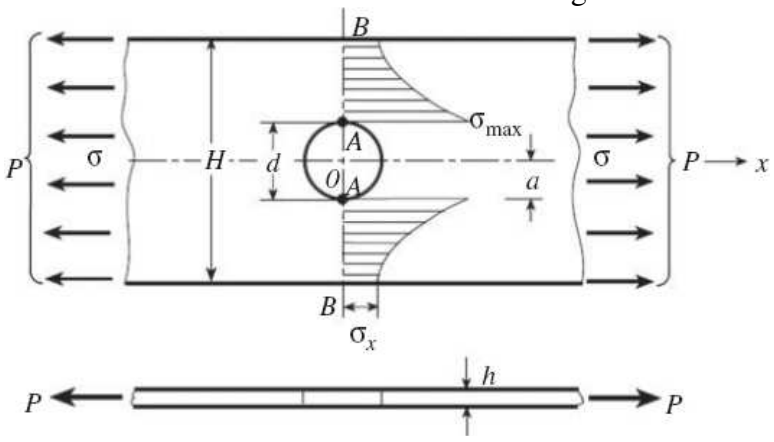

Figure 1. Tensile stress distribution around the hole in a plate with central hole.
Source: Pilkey et al. (2020).

The width of the plate is represented by H; d is the hole diameter, P is the tensile loading magnitude, a is the hole radius, h is the thickness, B is the farthest point in the width from the center of the hole, and O is the center of the hole. The stress distribution is also shown for the critical cross-section as a result of application of loading P (which generates the stress field σ in the region of application), highlighting σ_x (the minimum at the critical cross-

Revista Tecnológica - Universidade Estadual de Maringá - ISSN 1517-8048
DOI: 10.4025/revtecnol.v29i2.52653

section), and σ_{max}, which occurs at point *A*. This example addresses the following nominal stress (Equation 12) and the corresponding FSCF (Equation 13):

$$\sigma_{nomn} = \frac{P}{A_n} = \frac{P}{(H-d)h}\ ; \tag{12}$$

$$K_{tn} = \frac{\sigma_{max}}{\sigma_{nomn}} = \frac{\sigma_{max}(H-d)h}{P}. \tag{13}$$

Within the context of the plate with central hole, Equations 4 and 5 can be translated into second- and third-order polynomials, respectively, Equations 14 and 15 (both introduced by Howland, 1930), which were proposed to be based on interpolations performed over the experimental data gathered.

$$K_{tg} = 0.284 + 2\left(1-\frac{d}{H}\right)^{-1} - 0.600\left(1-\frac{d}{H}\right) + 1.32\left(1-\frac{d}{H}\right)^{2}; \tag{14}$$

$$K_{tn} = 2 + 0.284\left(1-\frac{d}{H}\right) - 0.600\left(1-\frac{d}{H}\right)^{2} + 1.32\left(1-\frac{d}{H}\right)^{3}. \tag{15}$$

In what concerns experimental values, Figure 2 shows them represented by curves related to the two different FSCFs, where the dashed line indicates extrapolation.

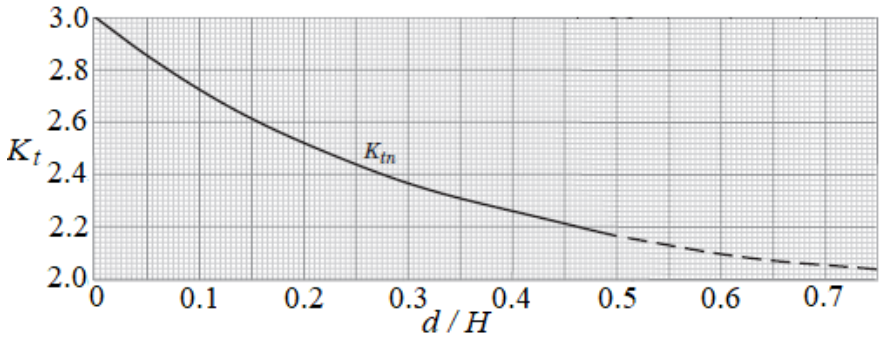

Figure 2. FSCFK_{tn} related to the geometric factor *d/H* for a plate with central hole in tension.**Source:** Howland (1930).

Therefore, related to the plate with central hole, the interpolated equation to calculate the FSCFs is obtained by the calculation of the coefficients from the linear system presented in Equation 9. The points $(x_i\ , y_i)$ entered as input for Equation 9 are the following: (0.000, 3.004); (0.100, 2.732); (0.200, 2.519); (0.300, 2.358); (0.400, 2.240); (0.500, 2.157); (0.600, 2.102); (0.700, 2.067); (0.800, 2.043). This yields Equation 16, which is applied directly in the software:

$$P(x) = -3.849\cdot 10^{-11}x^8 + 1.215\cdot 10^{-10}x^7 - 1.564\cdot 10^{-10}x^6 + 1.056 \cdot 10^{-10}x^5 - 4.011\cdot 10^{-11}x^4 - 1.320x^3 + 3.360x^2 - 3.044x + 3.004\,. \tag{16}$$

2.4Plate with Lateral Grooves Symmetrically Disposed

Another example often available in what concerns experimental points and commonly found in engineering design is the plate with opposite semicircular edge notches subjected to a uniform tensile loading system (see Figure 3).

Revista Tecnológica - Universidade Estadual de Maringá - ISSN 1517-8048
DOI: 10.4025/revtecnol.v29i2.52653

In Figure 3, H represents the width, the magnitude of the tensile loading system is P, the radius of both semi-circular notches is r, and the plate thickness is h. Consequently, the relation $H - 2r = d$ holds. Thus, σ_{nomg} is the same as obtained in Equation 5, and σ_{nomn} is given by Equation 17:

$$\sigma_{nomn} = \frac{P}{hd}. \tag{17}$$

Therefore, K_{tg} is the same as Equation 7, and K_{tn} results in Equation 18:

$$K_{tn} = \frac{\sigma_{max}}{\sigma_{nomn}} = \frac{\sigma_{max} hd}{P}. \tag{18}$$

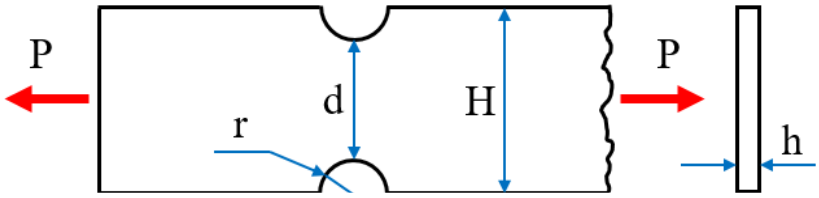

Figure 3. Strip weakened by symmetrical semi-circular notches.**Source:** Pilkey et al. (2020).

Equation 19 presents the approximate mathematical expression that represents the continuity of the experimental points obtained for the FSCF (Ling,1968). Similarly to the Equation 15, Equation 19 was also obtained by the author performing a cubic interpolation of the related experimental data.

$$K_{tn} = 3.065 - 3.472\left(\frac{2r}{H}\right) + 1.009\left(\frac{2r}{H}\right)^2 + 0.405\left(\frac{2r}{H}\right)^3. \tag{19}$$

Figure 4 shows the FSCF behavior related to the geometric parameter $2r / H$ for a plate with opposite semi-circular notches under tension.

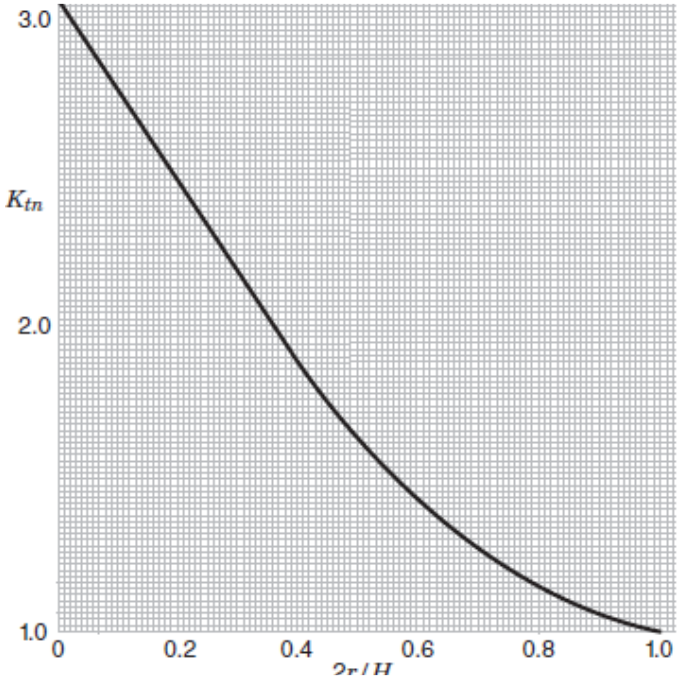

Figure 4. FSCF K_{tn} related to the geometric factor $2r/ H$ of a plate with opposite semi-circular edge in tension.**Source:** Ling (1968).

Revista Tecnológica - Universidade Estadual de Maringá - ISSN 1517-8048
DOI: 10.4025/revtecnol.v29i2.52653

Equation 20establishes the interpolated equation for the FSCF of the plate with opposite semi-circular edge in tension, obtained analogously to Equation 16, which is also within the developed software. The points $(x_i\,, y_i)$ entered as input for Equation 9 for this case are the following: (0.000, 3.065); (0.100, 2.728); (0.200, 2.414); (0.300, 2.125); (0.400, 1.864); (0.500, 1.632); (0.600, 1.433); (0.700, 1.268); (0.800, 1.141).

$$P(x) = 6.513 \cdot 10^{-11}x^8 - 2.043 \cdot 10^{-10}x^7 + 2.619 \cdot 10^{-10}x^6 - 1.766 \cdot 10^{-10}x^5 + 6.700 \cdot 10^{-11}x^4 + 0.405x^3 + 1.009x^2 - 3.472x + 3.065\,. \quad (20)$$

2.5Software Solution for FSCFs

The software developed and introduced here has the purpose of calculating the FSCF, nominal stress, and maximum stress for two types of discontinuities in plates under tension. Its graphical interface is shown in Figure 5.

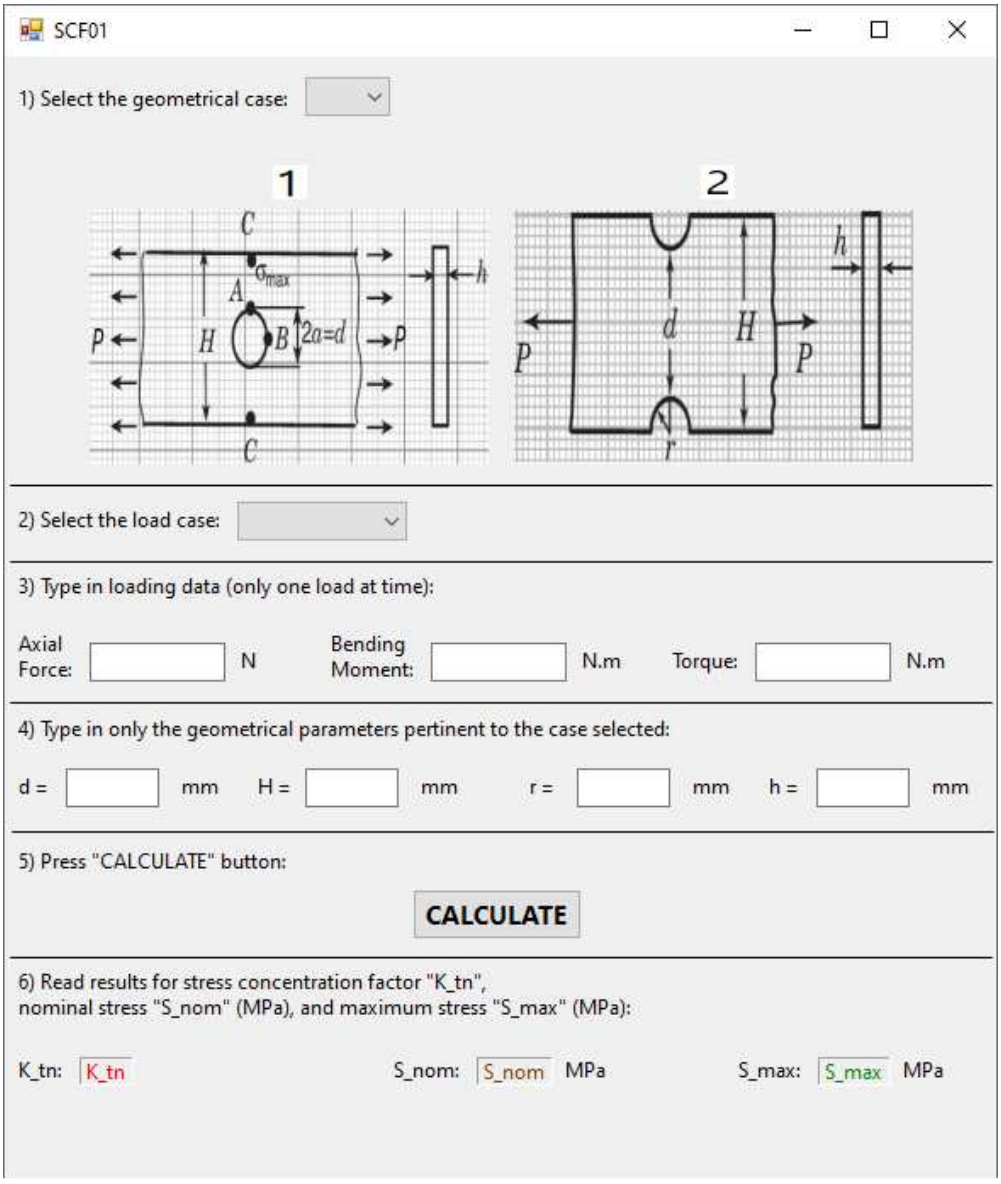

Figure 5. Graphical interface of the software. **Source:** the author (2020).

Revista Tecnológica - Universidade Estadual de Maringá - ISSN 1517-8048
DOI: 10.4025/revtecnol.v29i2.52653

The computer program consists of a Microsoft Windows®-based software, developed in Microsoft Visual Studio 10.0® by means of emulating the Microsoft Visual Basic 6.0® ambient.It is proposed to replace the well-known tables, charts, and expensive commercial packages in the calculation of the FSCFs of the cases and ranges covered. The referred software is capable of providing two sets of geometrical and tensile loading situations. In addition to the calculation of the FSCFs, the program presents the nominal and the maximum stresses for both cases.

From the point of view of computer program external architecture, the software is composed of drop-down boxes, text-boxes, instruction lines, illustrations, result-boxes, and a button. With regard to its internal structure, an adequate sequence of interpolation and stress equations, conditional statements, definition and attribution of variables, etc. is arranged.

The first four regions are related to the input data, which involves, respectively: (1) selection of the geometrical case (1 for plate with central hole under uniform tension; 2 for the case of plate with opposite semi-circular edge notches), (2) selection of the load case (only axial tension option is already available), (3) filling in the loading type field (magnitude in N), and (4) filling in the fields corresponding to the pertinent geometric variables (*d*, *H*, and *h* for the first case, and *H*, *r*, and *h* for the second case, all in mm).

The fifth section is dedicated to simply pressing the button “calculate” in order to perform the calculation and the sixth section gives the following output data: FSCF, nominal stress (in MPa), and maximum stress (also in MPa).

The software collects the input data typed in by the user. If one of the pertinent fields is not selected or is not filled in properly, an error message arise with some guidance to correct the missing or wrong information. If the software is fed correctly, it will provide the output by calculating the FSCF using Equation 16 (first case) or 20 (second case); the nominal stress will be calculated by Equation 3; and the maximum stress is provided by Equation 7. The flowchart shown in Figure 6 intends to simplify the software workflow.

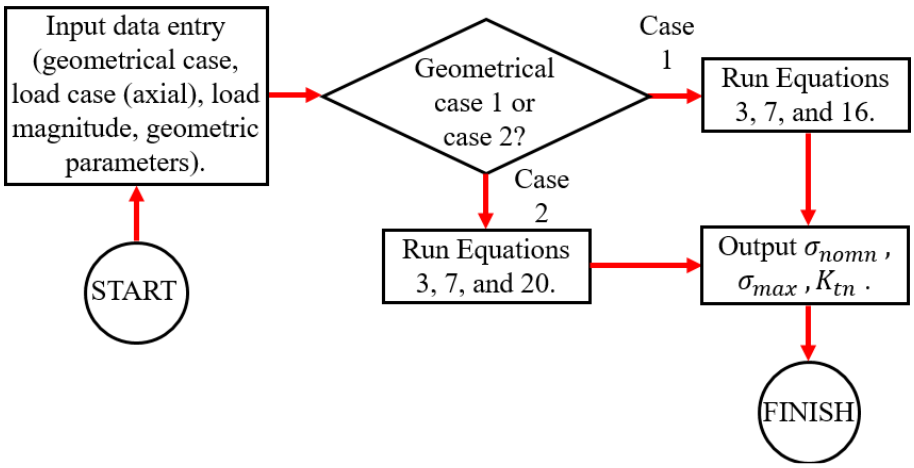

Figure 6. Workflow of the software. **Source:** the author (2020).

3 Validation of the Introduced Software (Results and Discussion)

This section presents the comparison of the results obtained from the developed software with those via chart reading and approximate equations proven for both cases studied. The validation is made by relating FSCFs from the software and from the equations mentioned.

Revista Tecnológica - Universidade Estadual de Maringá - ISSN 1517-8048
DOI: 10.4025/revtecnol.v29i2.52653

Table 1 evidences the comparison of all FSCFs obtained for the first case of discontinuity: the one collected by the simple reading process of the Figure 2corresponds to the second column, the other calculated by the application of Howland's equation (third column), and the one extracted from the software developed (forth column). The last column of Table 1 is the result of calculation of the relative error between values obtained via software and from chart reading.There is an agreement at least to the third decimal place between the results obtained by Howland's equation and those from the software, which, for the range of geometric factor *d / H* presented in the table, validates the software related to the precision mentioned for the application of the first case.

Table 1. First case: comparison between FSCFs from chart reading, from Howland's equation, and from software and the relative error

COMPARISON (FIRST CASE)				
d/H	FSCF FROM CHART	FSCF FROM HOWLAND'S EQUATION	FSCF FROM SOFTWARE	RELATIVE ERROR (%)
0.00	3.000	3.004	3.004	0.133
0.05	2.850	2.860	2.860	0.350
0.10	2.720	2.732	2.732	0.439
0.15	2.620	2.619	2.619	0.038
0.20	2.520	2.519	2.519	0.040
0.25	2.440	2.432	2.432	0.329
0.30	2.360	2.538	2.358	0.085
0.35	2.300	2.294	2.294	0.262
0.40	2.280	2.240	2.240	1.786
0.45	2.220	2.194	2.194	1.185
0.50	2.160	2.157	2.157	0.139
0.55	2.120	2.127	2.127	0.329
0.60	2.100	2.102	2.102	0.095
0.65	2.080	2.082	2.082	0.096
0.70	2.060	2.067	2.067	0.339
0.75	2.040	2.054	2.054	0.682

Source: the author (2020).

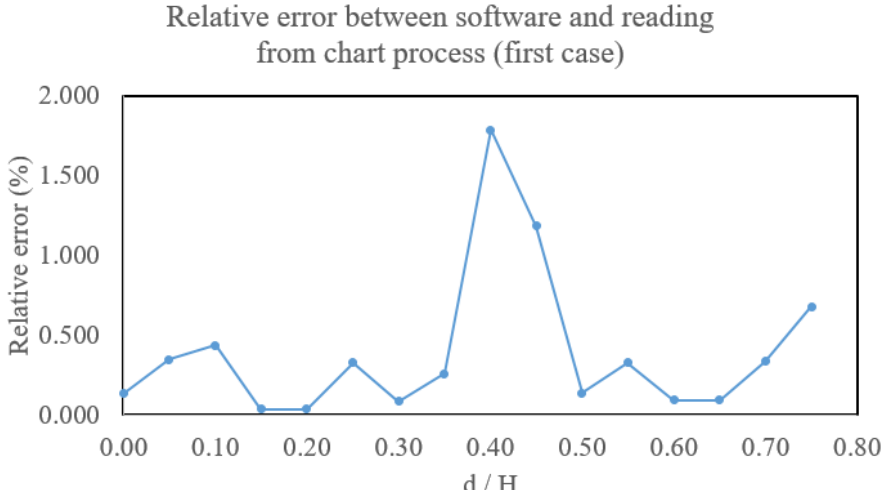

Figure 7. First case: relative error between software output FSCFs and factors obtained via reading process from chart.**Source:** the author (2020).

Revista Tecnológica - Universidade Estadual de Maringá - ISSN 1517-8048
DOI: 10.4025/revtecnol.v29i2.52653

In what concerns the difference between software output and values collected when reading the chart, a relative error was verified with its maximum occurring at d / H = 0.40 (relative error of 1.786%) and its minimum at d / H = 0.15 (relative error of 0.038%). Figure 7 presents this difference in a graphical manner. The discrepancies presented here are mainly due to the parallax error when one tries to extract a value of FSCF from the chart. Therefore, in the process of reading, the FSCF can be lower (hiding a higher real maximum stress) or higher (hiding a lower real maximum stress) than the value obtained via equation or software.

The discrepancies between FSCFs from reading the chart and from the software for the first case are presented in Figure 8 by the two curves.

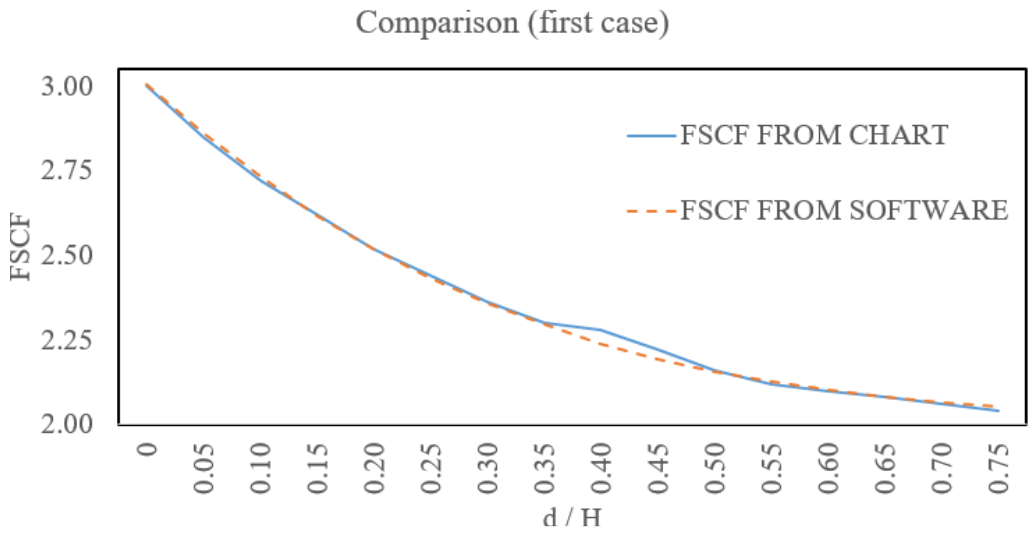

Figure 8. First case: comparison corresponding to Table 1.**Source:** the author (2020).

Analogously to Table 1, Table 2 compares all FSCFs obtained for the second case of discontinuity, one from chart, other from Ling's equation (Ling, 1968), and other from the developed software. Besides that, the relative error between values obtained via software and from chart reading are presented.

As verified for the first case, the validation of the software in the range of geometric factor $2r / H$ related to the second case could be achieved by the exact agreement until the third decimal place between the results obtained by Ling's equation and those from the software.

Values of FSCFs via reading and via software presented discrepancies along the range of geometric factor $2r / H$ covered. Its maximum occurred at $2r / H = 0.30$ (relative error of 2.588%) and its minimum at $2r / H = 0.75$ (relative error of 0.083%). An exception occurs at $2r / H = 0.60$, in which the compared values are equal until the second decimal place.It can be graphically checked in Figure 9. Similarly to the analysis made for the first case, this variation is predominantly explained by the parallax error in the extraction of FSCFs from the chart, presenting the same consequences as already described in the first case.

Revista Tecnológica - Universidade Estadual de Maringá - ISSN 1517-8048
DOI: 10.4025/revtecnol.v29i2.52653

Table 2. Second case: comparison between FSCF from chart reading, from Ling's equation, and from software and the relative error

COMPARISON (SECOND CASE)				
2r/H	FSCF FROM CHART	FSCF FROM LING'S EQUATION	FSCF FROM SOFTWARE	RELATIVE ERROR (%)
0.00	3.060	3.065	3.065	0.163
0.05	2.900	2.894	2.894	0.207
0.10	2.760	2.728	2.728	1.173
0.15	2.600	2.568	2.568	1.246
0.20	2.460	2.414	2.414	1.906
0.25	2.320	2.266	2.266	2.383
0.30	2.180	2.125	2.125	2.588
0.35	2.040	1.991	1.991	2.461
0.40	1.880	1.864	1.864	0.858
0.45	1.760	1.744	1.744	0.917
0.50	1.640	1.632	1.632	0.490
0.55	1.520	1.528	1.528	0.524
0.60	1.440	1.433	1.435	0.348
0.65	1.360	1.346	1.346	1.040
0.70	1.280	1.268	1.268	0.946
0.75	1.200	1.199	1.199	0.083
0.80	1.140	1.141	1.141	0.088
0.85	1.100	1.092	1.092	0.733
0.90	1.060	1.053	1.053	0.665
0.95	1.020	1.024	1.024	0.391

Source: the author (2020).

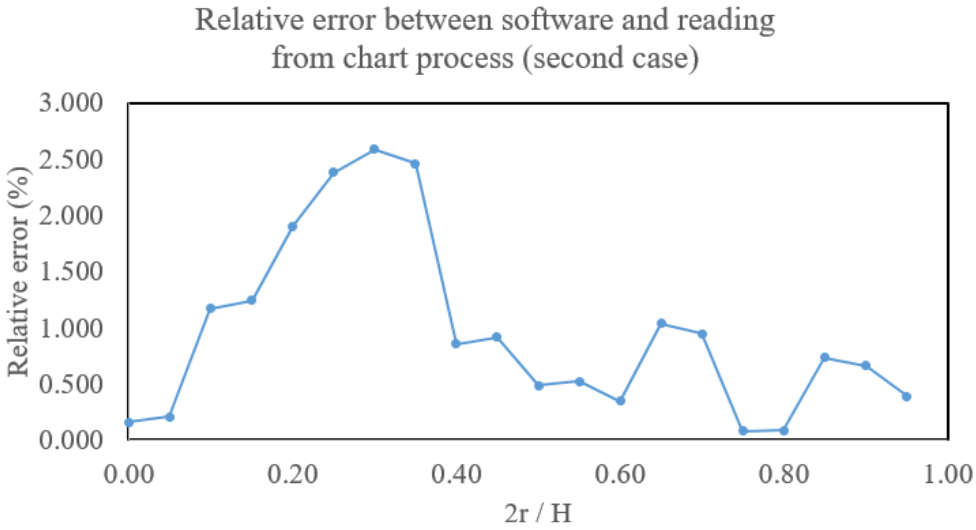

Figure 9. Second case: relative error between software output FSCFs and factors obtained via reading process.**Source:** the author (2020).

Figure 10 presents the described behavior related to the second case of discontinuity.

Revista Tecnológica - Universidade Estadual de Maringá - ISSN 1517-8048
DOI: 10.4025/revtecnol.v29i2.52653

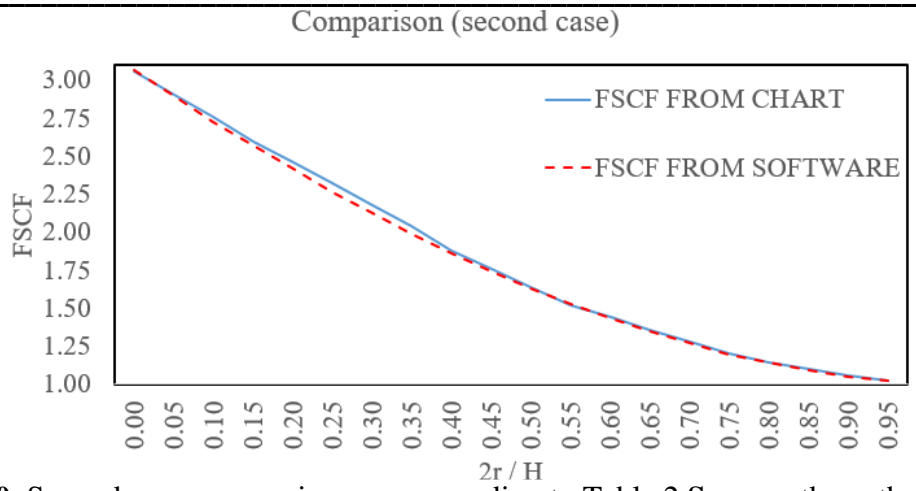

Figure 10. Second case: comparison corresponding to Table 2.**Source:** the author (2020).

In a general point of view, the results presented in Figures 8 and 10 present their corresponding critical regions, in which the discrepancy between data collected from chart and extracted from software are measured by the vertical distance between the curves.

4Conclusions

This paper presented the results of FSCFs for two geometrical cases of plates under tension in the elastic range. In addition, the program provided the user with the nominal and maximum stresses for both cases. Results provided by the software were validated through the comparison with the approximate equations from another authors and compared with the conventional reading process from charts.

For both cases covered by the software presented herein the interpolated equations used to model the curves resulted in good fit of data as proved by the comparison with another approximate equations, being able to be applied in the place of these proven equations.

For the first case of discontinuity calculated (with central hole), in general, the relative error presents lower magnitudes compared with the second case. This may be due to the fact that the second case presents a higher variation of the angular coefficient of the curve derivative (see Figures 2 and 4). This predisposes the second case to be more susceptible to higher errors in the process of reading the FSCFs.

Therefore, mainly due to the parallax error, the process of reading the FSCF directly from the adequate chart is not as accurate as obtaining it from an equation or from a validated software. Although it was not part of the scope of this software, the calculation of approximate equations of many situations of stress concentration phenomenon can be time consuming if it is not conducted through an organized manner, as the software proposes.

References

BIDHAR, S.; KUWAZURU, O.; SHIIHARA, Y.; UTSUNOMIYA, T.; HANGAI, Y.; NOMURA, M.; WATANABE, I.; YOSHIKAWA, N. Empirical formulation of stress concentration factor around an arbitrary-sized spherical dual-cavity system and its application to aluminum die castings. **Applied Mathematical Modelling**, v. 39, n. 1, p. 5707 – 5723, 2015.

Revista Tecnológica - Universidade Estadual de Maringá - ISSN 1517-8048
DOI: 10.4025/revtecnol.v29i2.52653

BUDYNAS, R. G.; NISBETT, J. K. **Shigley's mechanical engineering design.** 8.ed. New York: McGraw-Hill, 2008.

GUNWANT, D.; KSHETRI, R.; RAWAT, K.S. Determination of stress concentration factor in linearly elastic structures with different stress-raisers using FEM. **Int. Journal of Engineering Research and Application**, v. 6, n. 2, p. 29 – 35, 2016.

HOWLAND, R. C. J. On the stresses in the neighborhood of a circular hole in a strip under tension. **Philos, Trans. R. Soc.**, v. 229, n. 1, series A, p. 49 – 86, 1930.

JR, G. P.; SHAHHOSSEINI, A.M. Development of instructional software for the calculation of form stress concentration factors. **Computer Applications in Engineering Education**, v. 10, n. 1, p. 1 – 10, 2002.

KANNAN, R. **Fatigue assessment of offshore jacket structures: a case study**. 2018. 86p. Dissertation (Master's) – University of Stavanger, Stavanger.

KMECZ, G. M. **A study of the effect of drilled holes on the concentration of elastic stresses around a notch**. 1972. 93p. Dissertation (Master's) – Missouri University of Science and Technology, Rolla.

LING, C. B. On stress concentration factor in a notched strip. **Trans. ASME Appl. Mech. Sect.**, v. 35, n. 4, p. 833 – 835, 1968.

MUMINOVIC, A. J.; SARIC, I.; NEDZAD, R. Analysis of stress concentration factors using different computer software solutions. Proceedings of 24th DAAAM International Symposium on Intelligent Manufacturing and Automation.**Procedia Engineering**, v.69, n.1, p.609-615, 2014.

MUMINOVIC, A. J.; SARIC, I.; NEDZAD, R. Analysis of stress concentration factors using different computer software solutions. Proceedings of 24th DAAAM International Symposium on Intelligent Manufacturing and Automation.**Procedia Engineering**, v.100, n.1, p.707 – 713, 2015.

OZKAN, M. T.; TOKTAS, I. Determination of the stress concentration factor (K_t) in a rectangular plate with a hole under tensile stress using different methods. **Fracture Mechanics and Modelling**, v. 58, n. 10, p. 839 – 847, 2016.

PATHAK, R.; GIRI, N.; THAKUR, M.; PRAMOD, K. C.; UPRETY, S. Determination of stress concentration factor by different methods. **International Journal of Engineering Research & Technology**, v. 7, n. 08, p. 218 – 224, 2018.

PILKEY, W. D.; PILKEY, D. F.; BI, Z. **Peterson's stress concentration factors.** 4.ed. Hoboken: John Wiley & Sons, 2020.

SANTOS, A.; GUZMAN, R.; RAMIREZ, Z.; CARDENAS, C. Simulation of stress concentration factors in combined discontinuities on flat plates. **Journal of Physics: conference series**, v. 743, n. 1, p. 1 – 6, 2016.

YOUNG, W. C.; BUDYNAS, R. G. **Roark's formulas for stress and strain.** 7.ed. New York: McGraw-Hill, 2002.